EUROPEAN ORGANIZATION FOR NUCLEAR RESEARCH

INCLUSIVE ρ^0 PRODUCTION IN PP COLLISIONS AT THE CERN ISR

M.G. Albrow[1], S. Almehed[2], P.S.L. Booth[3], X. de Bouard[4], H. Bøggild[5], L.J. Carroll[3], P. Catz[4], E. Dahl-Jensen[5], I. Dahl-Jensen[5], G. Damgaard[5], G. von Dardel[2], N. Elverhaug[6], K.H. Hansen[5], J.N. Jackson[3], G. Jancso[4*], G. Jarlskog[2], H.B. Jensen[5], L. Jönsson[2], A. Klovning[6], E. Lillethun[6], A. Lu[4], B. Lörstad[2], N.A. McCubbin[1], A. Melin[2], H.E. Miettinen[5], R. Møller[5], B.S. Nielsen[5], S.Ø. Nielsen[5], J.O. Petersen[5], J.A.J. Skard[6], P. Villeneuve[7]

British-French-Scandinavian Collaboration

1) Rutherford Laboratory, Chilton, Didcot, United Kingdom

2) University of Lund, Sweden

3) University of Liverpool, United Kingdom

4) Laboratoire d'Annecy-le-Vieux de Physique des Particules, Annecy, France

5) Niels Bohr Institute, Copenhagen, Denmark

6) University of Bergen, Norway

7) LPHNE, University of Paris VI, Paris, France

Geneva, December 1978

(Submitted to Nuclear Physics B)

---

*) Now at the Central Research Institute for Physics, Hungerian Academy of Sciences, Budapest

Abstract

The inclusive production of ρ^0 mesons in pp collisions has been measured at five c.m. energies from $\sqrt{s}$ = 23.6 to 63.0 GeV. The cross-sections and the production spectra as a function of transverse momentum and rapidity are discussed.

1. Introduction

Recent experiments have indicated a significant production of resonances in high energy hadron collisions[1,2]. These results are of interest because of their interpretation in terms of the quark model of hadronic matter. For instance, arguments based on spin statistics suggest that the majority of all observed particles may be the decay products of meson resonances[3]. A more sophisticated approach in terms of the quark fusion model[4] has been shown to provide a quantitative description of the inclusive vector meson spectra for which data exist.

In this paper, we describe the results of a study of the inclusive production of ρ^0 mesons in proton-proton collisions at five c.m. energies, $\sqrt{s}$ = 23.6, 30.6, 44.6, 52.8 and 63.0 GeV, at the CERN ISR using data taken for calibration purposes during an experiment investigating high p_T phenomena. In a previous paper[2], we have presented an analysis of the data at $\sqrt{s}$ = 52.8 GeV using a different technique, which gave a significantly larger estimate of the number of ρ^0 mesons per inelastic event. The limitations of both analyses are discussed.

The paper is organized as follows. The apparatus and data reduction are described in Section 2, followed by a discussion of the experimental acceptance in Section 3. The results are presented in Section 4. Section 5 contains a summary of the conclusions.

2. Apparatus and Data Reduction

The experiment was carried out using the Split Field Magnet (SFM) and its detector of multi-wire proportional chambers. Figure 1 is a schematic drawing of the detector. A detailed description of the facility can be found elsewhere[5].

The data were taken with the detector in a self-triggering mode, in which at least two charged tracks were required anywhere in the chambers. In this mode about 95% of the inelastic events triggered the detector.

2.1 Variables

The events are described in a right-handed Cartesian coordinate system, where the x-axis is pointing radially outwards from the ISR centre, the y-axis is the bisector of the acute angle between the beams, and the z-axis is pointing vertically upwards. In the c.m.s. of the collision, the y-axis is along the beams.

All the following variables are defined in the c.m.s.

$\vec{p} = (p_x, p_y, p_z)$ is the momentum vector of a particle.

$p_T = \sqrt{p_x^2 + p_z^2}$ is the transverse momentum.

$x = 2\, p_y/\sqrt{s}$ is the Feynman scaling variable.

$y = \frac{1}{2} \ln \frac{E + p_y}{E - p_y}$ is the longitudinal rapidity where $E = \sqrt{\vec{p}^2 + m^2}$.

ϕ is the azimuth angle around the beam direction with $\phi = 0$ in the direction of the positive x-axis and $-180^\circ < \phi < 180^\circ$.

θ is the polar angle measured from the y-axis.

$\eta = -\ln \tan \theta/2$ is the pseudo - rapidity.

2.2 Data reduction

For each event recorded, modified versions of the SFM pattern recognition and geometry programs MARC and NICOLE[6] were used to reconstruct the charged particle tracks, fit them to a common vertex and determine the particle momenta. Events with only two positive tracks, both with $|x| > 0.85$, were found to be due mainly to elastic scattering and were removed from the sample. The remaining data sample consisted of about 25000 events at each energy.

In each event, the particles were treated as pions and their momenta transformed to the c.m.s. Positive particles with $|x| > 0.4$ have a high probability (> 80%) of being protons and were not used in the subsequent analysis.

3. Acceptance

Due to the geometry of the detector and the SFM field configuration, the acceptance of the detector and the fractional error in the measured laboratory momentum, $(\Delta p/p)_{lab}$, vary considerably with the particle direction and momentum. To achieve a mass resolution of < 5% over the whole mass range only tracks with $(\Delta p/p)_{lab} < 0.3$ and $|\vec{p}| > 0.3$ GeV/c were used in constructing the two-pion effective mass spectrum.

3.1 Single particle acceptance

The acceptance for single particles was determined as a function of their charge, η, ϕ and p_T using a Monte Carlo technique. Events were generated with realistic vertex, multiplicity, y, ϕ and p_T distributions. The particles were tracked through the field and the trajectories digitized to simulate the detector output. An ideal detector with no misalignments and 100% efficiencies was assumed. The resulting simulated data were processed by the program chain.

For particles with $(\Delta p/p)_{lab} < 0.3$, acceptance tables were generated with bin sizes, $\Delta\phi = 10^{o}$, $\Delta\eta = 0.2$ for both charges and the three ranges of transverse momentum, $0.0 < p_T < 0.2$ GeV/c, $0.2 < p_T < 0.4$ GeV/c and $p_T > 0.4$ GeV/c. The statistical error per bin was typically better than 10%, except in the forward region. Consequently only particles with $|\eta| < 3.4$ were included in the subsequent analysis. Figure 2 illustrates the acceptance for particle trajectories with $(\Delta p/p)_{lab} < 0.3$ as a function of $|\phi|$ for several ranges of p_T and η. The detector is symmetric about the horizontal plane and thus $|\phi|$ can be used rather than ϕ. With the cuts mentioned above about 40% of the charged particles produced in an inelastic event were accepted.

We have checked that folding the acceptance into the measured inclusive cross-sections[7] reproduces the particle distributions observed in the detector at $\sqrt{s} = 52.8$ GeV. At all energies the multiplicity of negative particles, calculated from the observed multiplicity and the acceptance, agrees well with the values obtained from previous ISR experiments[8].

3.2 Rho meson acceptance

Neutral ρ mesons were generated with a P-wave Breit-Wigner mass distribution given by Roos[9]. The ρ^0 mesons were assumed to be produced unpolarized with y and p_T distributions consistent with the measured differential cross-sections quoted later. The momenta of the decay pions were smeared with the detector resolution. If both pions satisfied the same cuts as imposed on the data, the efficiency for the detection of the generated ρ^0 meson was taken to be the product of the acceptance of the pions derived from the tables. The probability of detecting a ρ^0 meson varied from 0.13 at $\sqrt{s} = 23.6$ GeV to 0.21 at 63.0 GeV due mainly to the

reduced magnetic field at the lower energies. The acceptance varied by a factor of two across the y range but was insensitive to the transverse momentum.

4. Analysis and Results

After applying the cuts described above to the data, the mass distribution of all possible $\pi^+\pi^-$ combinations in each event was formed. This distribution for the data at $\sqrt{s}$ = 52.8 GeV is shown in figure 3a. To remove the combinatorial background from this plot, a spectrum of uncorrelated $\pi^+\pi^-$ pairs was constructed by combining pions from one event with pions from other events. The uncorrelated background spectrum generated in this way and normalized to the mass distributions in figure 3a in the mass range from 2 to 4 GeV/c^2, where the correlations are expected to be negligible, is shown in figure 3b. A Monte Carlo prediction calculated from the measured pion inclusive distributions[7] weighted by the acceptance is also shown in this figure and is in good agreement with the uncorrelated spectrum. The difference between the spectra of figures 3a and 3b is taken to be the correlated spectrum and is shown in figure 4a.

In a previous paper[2] we have interpreted this correlated spectrum at $\sqrt{s}$ = 52.8 GeV as arising from the decay of vector mesons, principally the ρ^0, ω and K* (890) where the kaon has been misidentified as a pion. By comparison, in other experiments[10-13] at lower energies, two pion mass spectra such as that in figure 3a have been analysed by assuming the enhancement around 0.75 GeV/c^2 to be due to the ρ^0 meson and the signal then extracted by fitting to a Breit-Wigner mass distribution plus a polynomial background. Both these techniques have their short-comings. On the one hand, our earlier method neglects the contributions from higher mass resonances decaying into three or more particles and hence

overestimates the contribution from the vector mesons. In particular it yields a K* contribution five times larger than the upper limit obtained in a recent FNAL bubble chamber experiment at $\sqrt{s}$ = 19.7 GeV[14]. In addition, the ρ^0 meson signal observed is significantly larger than would be expected from an extrapolation of the lower energy data obtained using the polynomial background method. On the other hand, it has recently been pointed out[15] that this latter method may underestimate the ρ^0 signal because ignoring the contribution of the ω decay products to the low mass part of the two pion spectrum leads to an overestimation of the polynomial background under the ρ^0 meson.

In this paper, in order to compare our data with the lower energy data, we extract the ρ^0 signal by fitting the observed correlated spectrum around the ρ^0 mass with a P-wave Breit-Wigner distribution plus a mass dependent background function. It has been pointed out[16] that, based on a Mueller-Regge approach, the correlation function should vary inversely as the mass m of the pion pair at high masses. We find that a two parameter function of the form $a_1/m + a_2/m^2$ gives an acceptable fit to the background. The fit was carried out in the mass range 0.5 to 1.5 GeV/c^2 using values for the ρ^0 meson parameters of m_ρ = 740 MeV and Γ_ρ = 160 MeV. These values were obtained by fitting the data at the higher ISR energies where the signal is largest. The fit at $\sqrt{s}$ = 52.8 GeV is shown superimposed on the data in figure 4a, while figure 4b shows the equivalent correlated spectrum and fit at $\sqrt{s}$ = 23.6 GeV, where the signal is weakest.

We have investigated the effect of different background parametrizations on the size of the observed ρ^0 signal. For example, we find that a background function of the form $a_1 \exp(-a_2 m)$ gives equally acceptable fits and reduces the observed signal by 25%. In the results that follow, the

errors quoted are purely statistical and correspond to a change of χ^2 of 1 as given by the fitting program MINUIT[17].

4.1 Total inclusive cross-sections

The mean number of ρ^0 mesons observed per inelastic event corrected for acceptance and the χ^2/NDF for the fits are given in Table 1, together with the total inclusive cross-sections. At $\sqrt{s}$ = 52.8 GeV the number of ρ^0 mesons per inelastic event obtained using the analysis described here is 0.68 ± 0.06 compared with a value of 1.19 ± 0.25 from our previous method[2]. The cross-sections, together with the data at lower energies, are plotted as a function of $\sqrt{s}$ in figure 5a. The line on this figure is a fit to all the data, of the form

$$\sigma_{inc} = a \ln^2 s + b$$

with a = 0.38 ± 0.02 mb, b = -2.1 ± 0.4 mb, s in GeV and χ^2/NDF = 6/8.

Table 1 also shows the $\sigma(\rho^0)/\sigma(\pi^-)$ ratios, which are plotted along with the data at lower energies in figure 5b. We have used the results of reference 8) to correct our negative particle yields for K^- and $\bar{p}$ contamination. The ratio shows little variation from a value of 0.14 over the ISR energy range.

4.2 Inclusive differential cross-section

The mass distributions of the $\pi^+\pi^-$ pairs have been studied in several intervals of the variables p_T and y, and the ρ^0 signals extracted. The fits had typically χ^2/NDF = 38/37 and the sum of the signals thus obtained was within half a standard deviation of the ρ^0 signal from the total sample.

The cross sections $d\sigma/dp_T^2$ are given in Table 2 for five ranges of p_T^2 and plotted in figure 6 as a function of p_T. The straight lines on the figure are the results of a fit of the form

$$d\sigma/dp_T^2 = A(s) \exp(-Bp_T^2)$$

to the data at all five c.m. energies. The fit had χ^2/NDF of 22/19 and the value of B was found to be 3.3 ± 0.2 $(GeV/c)^{-2}$, which is consistent with the values obtained for ρ^0 production in pp and $\pi^{\pm}p$ collisions at lower energies[1,10,12,13]. This yields $\langle p_T \rangle = 0.49 \pm 0.02$ GeV/c, to be compared with $\langle p_T \rangle \simeq 0.3$ GeV/c for pions.

Table 3 shows the cross-sections $d\sigma/dy$ for three ranges of $|y|$. In figure 7, the values of $d\sigma/dy$ at all energies are plotted as a function of $y_{lab} = y_{beam} - y$, where y_{beam} is the c.m. rapidity of an incident proton. Within the statistical variations, the data are consistent with scaling in the ISR energy range.

5. Conclusions

From this study of ρ^0 production in pp collisions in the energy range from $\sqrt{s} = 23.6$ to 63.0 GeV the following conclusions can be drawn:

i) The total inclusive cross-section rises as s increases such that our data and that at lower energies can be fitted by the form:

$$\sigma_{inc}(mb) = (0.38 \pm 0.02) \ln^2 s - (2.1 \pm 0.4)$$

ii) The ratio $\sigma(\rho^0)/\sigma(\pi^-)$ shows little variation from the value 0.14 over the ISR energy range.

iii) At all energies the p_T dependence out to 1.5 GeV/c is

well represented by the form:

$$d\sigma/dp_T^2 = A(s) \quad \exp\ (-3.3 \pm 0.2).\ p_T^2$$

where p_T is in GeV/c.

iv) The y_{lab} distributions show no significant deviations from scaling in the ISR energy. region.

With this method of extracting the ρ^0 signal, the uncertainty in background parametrization gives rise to ± 25% systematic error in the calculated cross-sections. However, this uncertainty in normalization does not affect the conclusions about the p_T and y distributions.

6. Acknowledgements

It is a pleasure to thank the SFM detector group and the staff of the ISR division at CERN for their help, and members of the CERN programming staff for their assistance in the on-line and off-line analysis. We would also like to thank J. Burger, Ph. Dam, B. Guillerminet, P. Herbsleb, J.E. Hooper, D. Korder, E. Lohse, J.V. Morris, T. Sanford, D.B. Smith and M-I. Sundell for their contribution and assistance. Some authors (S.A., X. deB., H.B.J., A.K., B.L., H.E.M., R.M. and P.V.) acknowledge financial support from CERN during part of the experiment.

We gratefully acknowledge support from the CERN, Rutherford and Daresbury computing facilities and from the computer centres at Copenhagen and Lund Universities. We also acknowledge the loan of electronics from the Laboratory for Nuclear Science of the Massachusetts Institute of Technology.

The experiment was supported by the United Kingdom Science Research Council, The Danish and Swedish Natural Science Research Councils, The Norwegian Research Council for Science and the Humanities, and L'Institut National de Physique Nucléaire et de Physique des Particules, France.

REFERENCES

1) J. Whitmore, Phys. Reports 27C (1976) 187 and references therein.

2) G. Jancso et al., Nucl. Phys. B124 (1977) 1.

3) V.V. Anosivich and V.M. Shekter, Nucl. Phys. B55 (1973) 455.
V.M. Shekter and L.M. Shcheglova, Yadern Fiz. 27, (1978) 1070.
(Sov. J. Nucl. Phys., to be published).

4) S. Nandi, V. Rittenberg and H.R. Schneider, Phys. Rev.D17 (1978) 1336.

5) R. Bouclier et al., Nucl. Instr. Methods 125 (1975) 19 and references therein.

6) A. Frölich et al., CERN/DD/76/5 (1976).
M. Metcalf et al., CERN 73-2 (1973).

7) M.G. Albrow et al., Nucl. Phys. B56 (1976) 333.
M.G. Albrow et al., Nucl. Phys. B73 (1974) 40.
B. Alper et al., Nucl. Phys. B100 (1975) 237.
P. Capiluppi et al., Nucl. Phys. B79 (1974) 189.
K. Guettler et al., Phys. Letters 64B (1976) 111.

8) A.M. Rossi et al., Nucl. Phys. B84 (1975) 267.

9) M. Roos, Nucl. Phys. B97 (1975) 165.

10) V. Blobel et al., Phys. Letters 48B (1974) 73.
V. Blobel et al., Nucl. Phys. B69 (1974) 454.

11) V.V. Ammosov et al., Yadern Fiz. 24 (1976) 59.

12) R. Singer et al., Phys. Letters 60B (1976) 385.

13) H. Kichimi et al., Contribution to Tokyo Conf. (1978).

14) R. Singer et al., Nucl. Phys. B135 (1978) 265.

15) N.S. Angelov et al., Sov. J. Nucl. Phys. 25 (1977) 63.

16) E.L. Berger et al., Phys. Rev. D15 (1977) 206.

17) F. James and M. Roos, CERN/DD/75/20.

Table 1

The mean number, $\langle n_{\rho^0} \rangle$, of ρ^0 mesons per inelastic event corrected for acceptance, the χ^2/NFD of the fit to the mass spectrum, the total inclusive cross-sections, σ_{inc}, for ρ^0 mesons and the $\sigma(\rho^0)/\sigma(\pi^-)$ ratio at the five c.m. energies.

	$\sqrt{s}$(GeV)				
	23.6	30.6	44.6	52.8	63.0
$\langle n_{\rho^0} \rangle$	0.38 ± 0.05	0.54 ± 0.06	0.59 ± 0.05	0.68 ± 0.06	0.59 ± 0.07
χ^2/NDF	30 / 37	29 / 37	58 / 37	37 / 37	39 / 37
σ_{inc}(mb)	12.4 ± 1.7	18.3 ± 2.2	20.6 ± 1.9	24.3 ± 2.1	20.9 ± 2.4
$\sigma(\rho^0)/\sigma(\pi^-)$	0.13 ± 0.02	0.16 ± 0.02	0.15 ± 0.02	0.15 ± 0.02	0.12 ± 0.02

Table 2

Differential cross-section for ρ^0 production, $d\sigma/d\ p_T^2$, in units of mb $(GeV/c)^{-2}$.

p_T range (GeV/c)	$< p_T^2 >$ $(GeV/c)^2$	$\sqrt{s}$ (GeV)				
		23.6	30.6	44.6	52.8	63.0
0.00 - 0.25	0.03	36 ± 9	49 ± 14	53 ± 10	74 ± 13	79 ± 13
0.25 - 0.50	0.15	24 ± 5	42 ± 7	43 ± 6	56 ± 7	36 ± 8
0.50 - 0.75	0.39	8.6 ± 3.4	16 ± 4	15 ± 3	16 ± 4	16 ± 4
0.75 - 1.00	0.76	3.6 ± 1.2	4.2 ± 1.6	5.7 ± 2.0	3.2 ± 1.6	6.4 ± 2.0
1.00 - 1.50	1.44	0.7 ± 0.4	0.5 ± 0.3	1.5 ± 0.4	1.1 ± 0.4	1.2 ± 0.5

Table 3

Differential cross-section for ρ^0 production, $d\sigma/dy$, in units of mb per unit y.

|y| range	$\sqrt{s}$ (GeV)				
	23.6	30.6	44.6	52.8	63.0
0 - 1	3.3 ± 0.9	4.3 ± 1.2	3.4 ± 0.8	3.0 ± 1.0	4.7 ± 1.0
1 - 2	1.8 ± 0.5	2.9 ± 0.6	3.5 ± 0.5	4.6 ± 0.6	3.4 ± 0.7
2 - 3	1.0 ± 0.2	1.5 ± 0.3	2.3 ± 0.3	2.7 ± 0.3	1.9 ± 0.4

Figure Captions

Fig. 1 : Schematic drawing of the SFM detector showing the multiwire proportional chambers of the central and one of the forward detectors. The upper pole piece and the other forward detector have been omitted for clarity.

Fig. 2 : The average fractional acceptance for positive and negative particles as a function of azimuthal angle $|\phi|$ for several ranges of η and p_T at the high field setting of the SFM.

Fig. 3 : Effective mass spectra for $\pi^+\pi^-$ at $\sqrt{s}$ = 52.8 GeV of a) all combinations within each event and b) uncorrelated pions from different events normalized to a) between 2 and 4 GeV/c^2.

The dashed curve in b) is a Monte Carlo prediction obtained by randomly combining pions generated with the measured single particle inclusive distributions. The acceptance and momentum resolution have been folded in and the spectrum normalized to the uncorrelated spectrum between 0 and 4 GeV/c^2.

Fig. 4a : The correlated spectrum at $\sqrt{s}$ = 52.8 GeV obtained by subtracting the spectrum of fig. 3b from 3a.

4b : The equivalent spectrum at $\sqrt{s}$ = 23.6 GeV.

In each case the full curve is the fit described in the text, while the dashed curve represents the background contribution.

Fig. 5a : The total inclusive cross-section for the production of ρ^0 mesons as a function of $\sqrt{s}$. The curve is the fit described in the text to all the data plotted.

5b : The ratio $\sigma(\rho^0)/\sigma(\pi^-)$ as a function of $\sqrt{s}$.

● This experiment, x Blobel et al[10]
◐ Amosov et al[11], ◙ Singer et al[12],
▽ Kichimi et al[13].

Fig. 6 : $d\sigma/dp_T^2$ versus p_T^2.

The lines are the results of the global fit to the data described in the text. The number attached to each line is the c.m. energy in GeV.

Fig. 7 : $d\sigma/dy$ versus $y_{lab} = y_{beam} - y$. The dashed line is the rapidity distribution assumed in the acceptance program, normalized to the mean value of $d\sigma/dy$ in the interval $|y| < 1$ at the three higher energies.

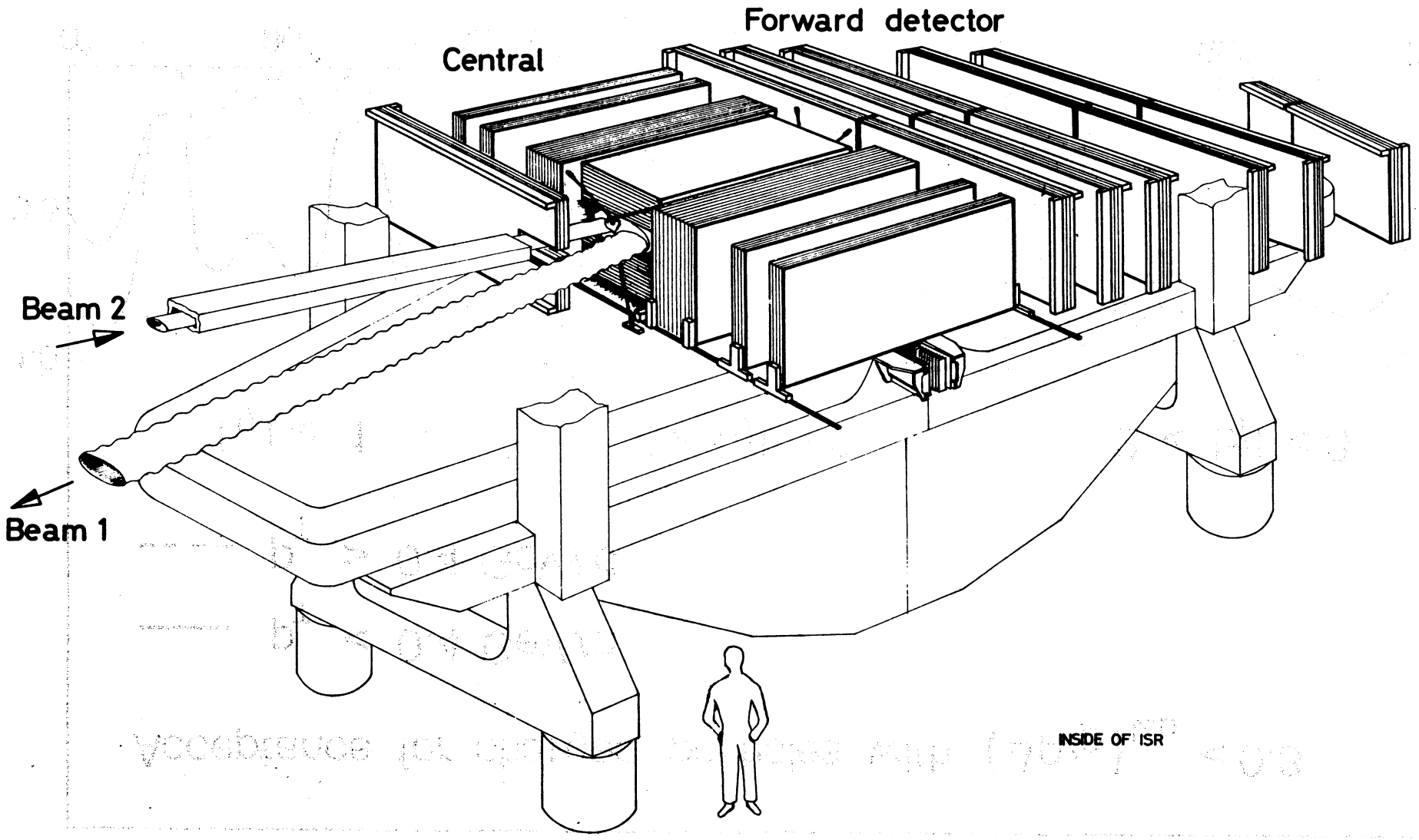

Fig. 1

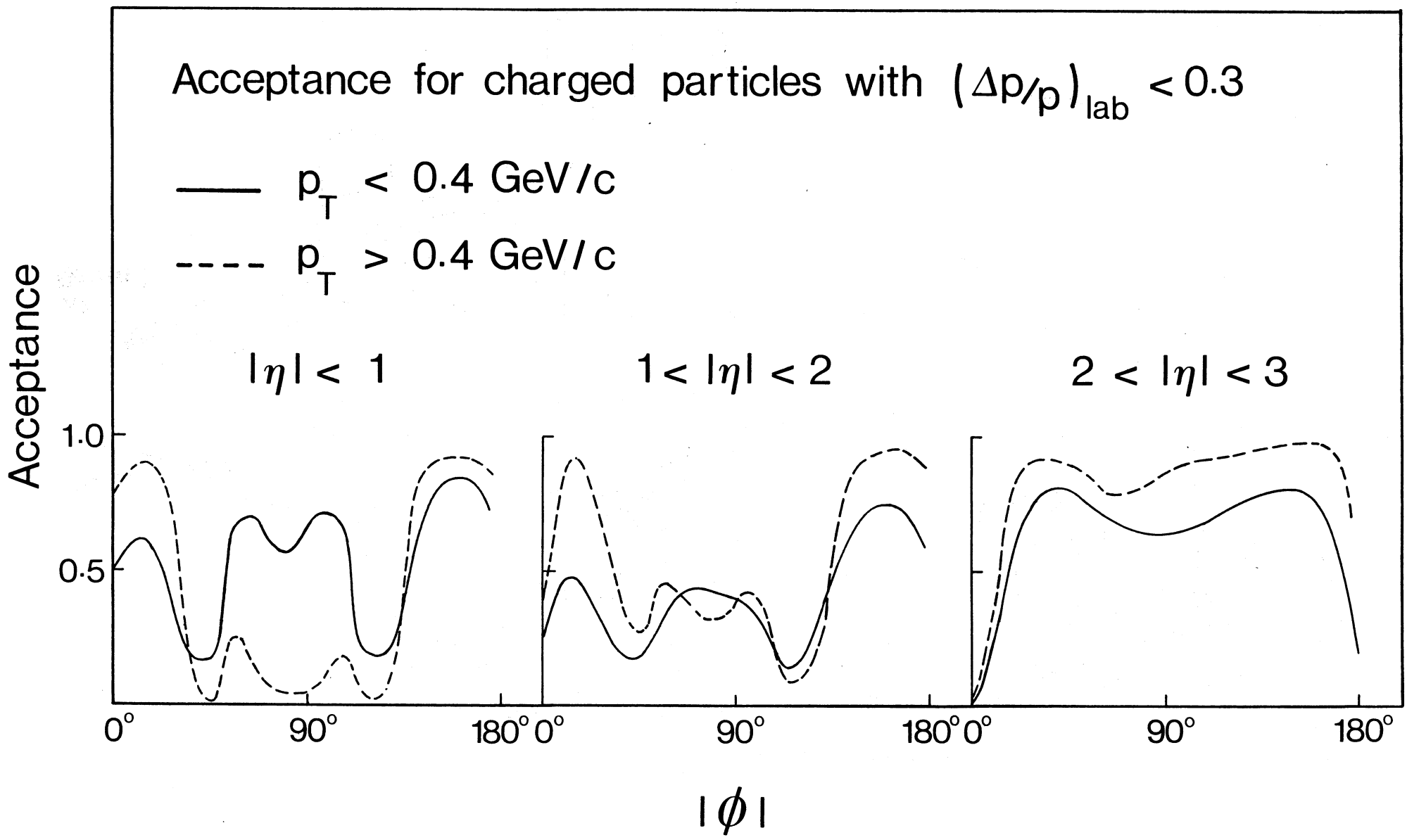
Acceptance for charged particles with $(\Delta p/p)_{lab} < 0.3$
—— $p_T < 0.4$ GeV/c
---- $p_T > 0.4$ GeV/c
$|\eta| < 1$
$1 < |\eta| < 2$
$2 < |\eta| < 3$
Acceptance
1.0
0.5
0°
90°
180°
$|\phi|$

Fig. 2

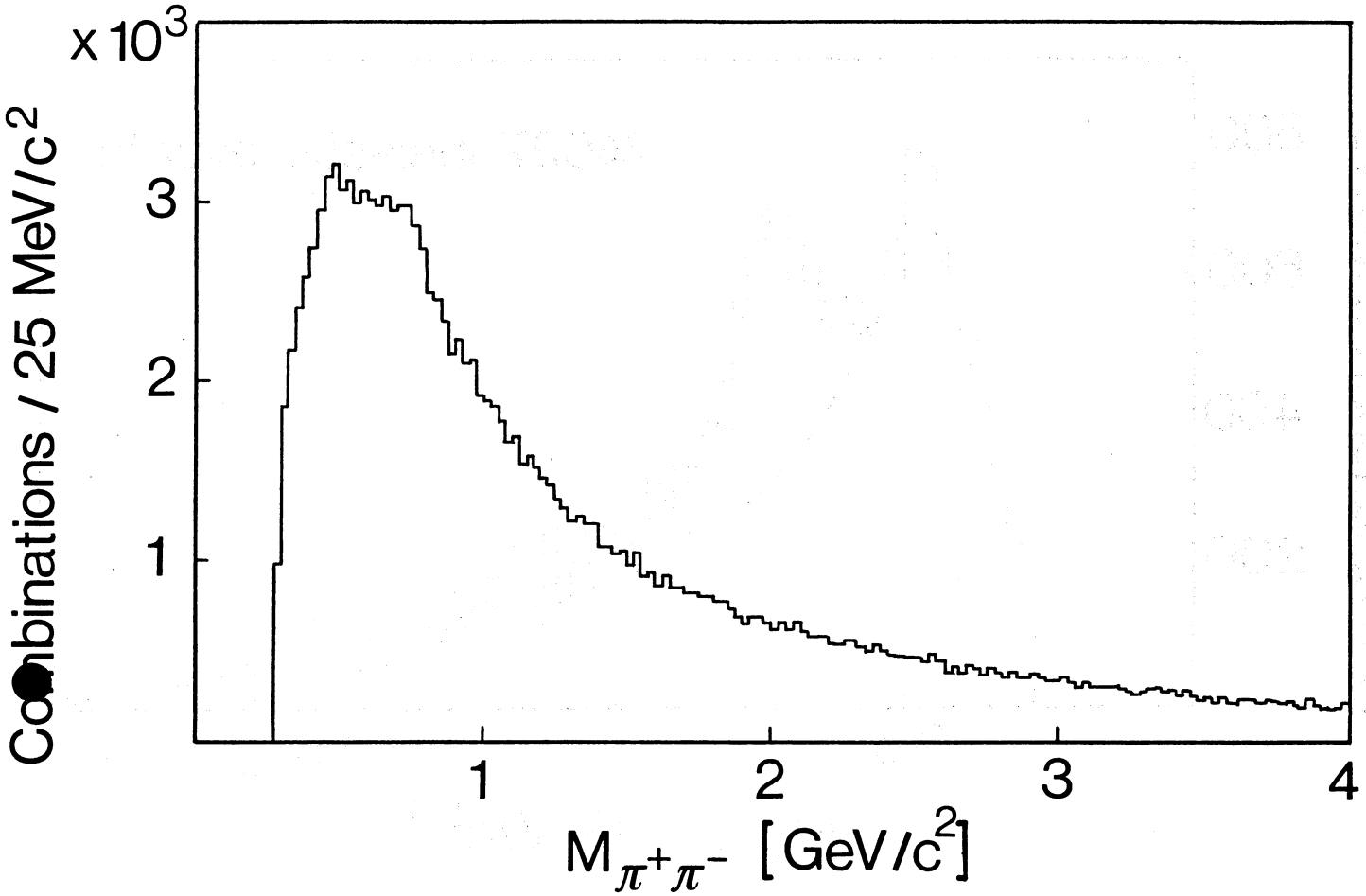
x 10^3
3
2
1
Combinations / 25 MeV/c^2
1
2
3
4
M_π+π- [GeV/c^2]

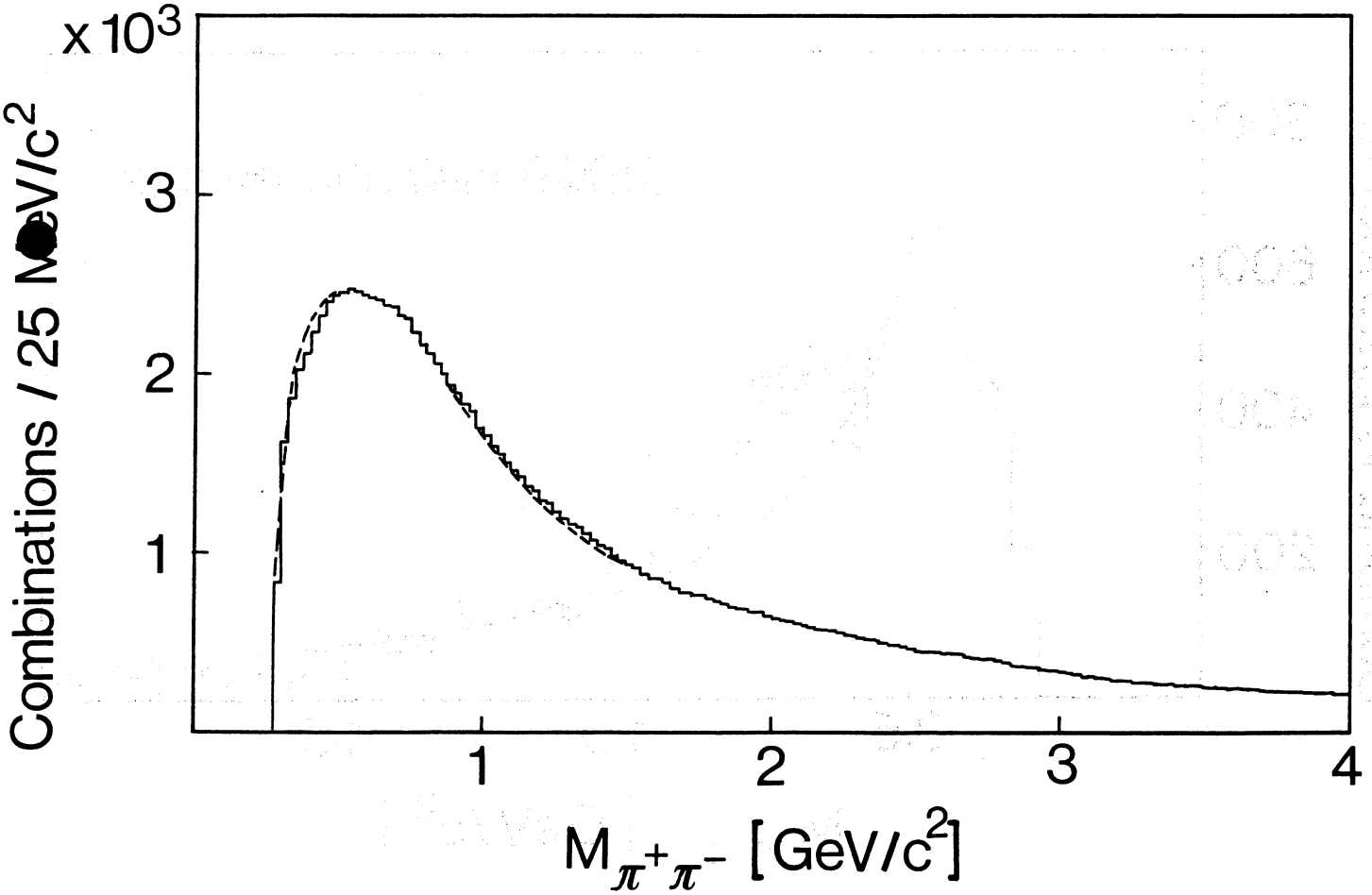
x 10^3
3
2
1
Combinations / 25 MeV/c^2
1
2
3
4
M_π+π- [GeV/c^2]

Fig. 3a.b

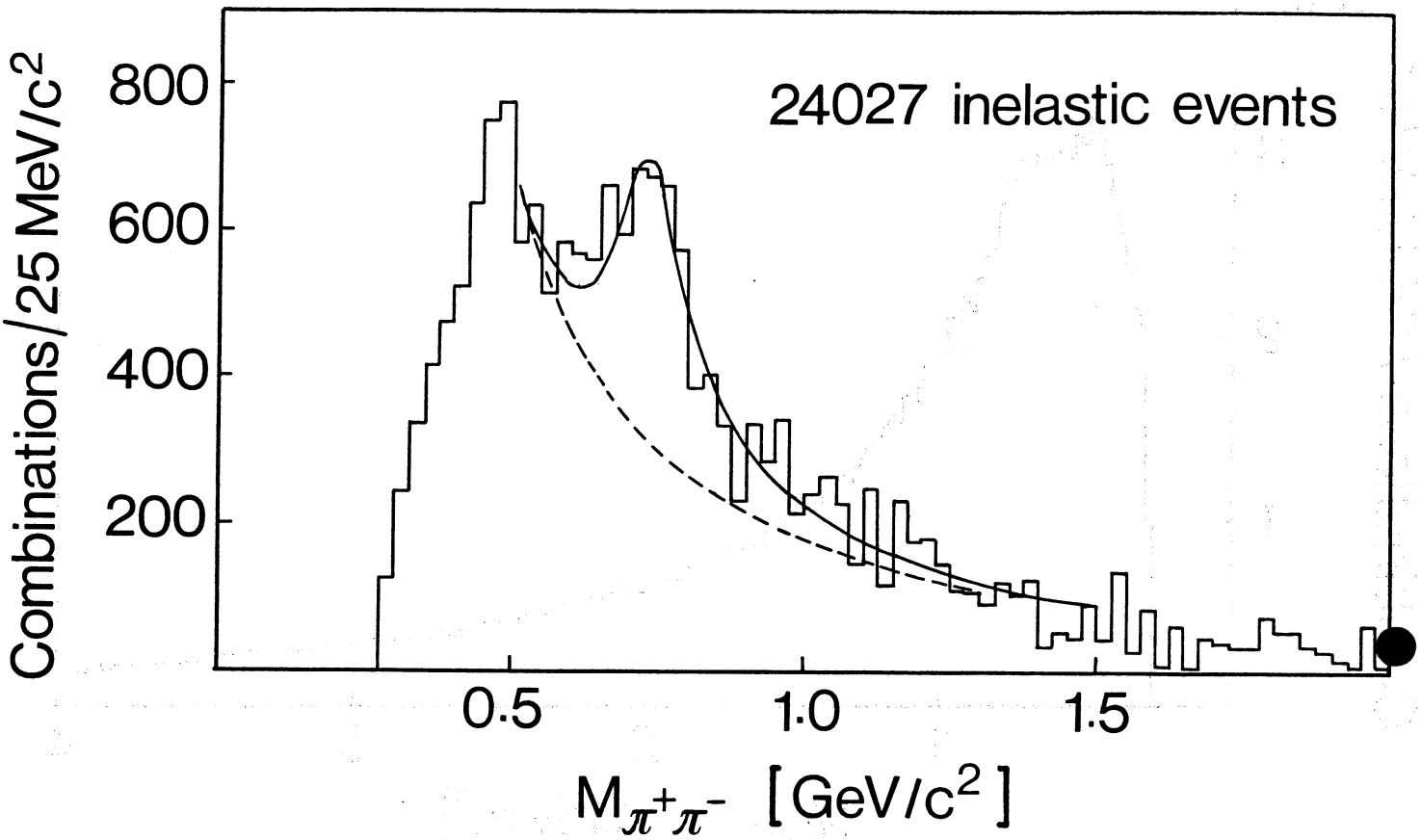
24027 inelastic events
Combinations/25 MeV/c²
800
600
400
200
0.5
1.0
1.5
M π⁺π⁻ [GeV/c²]

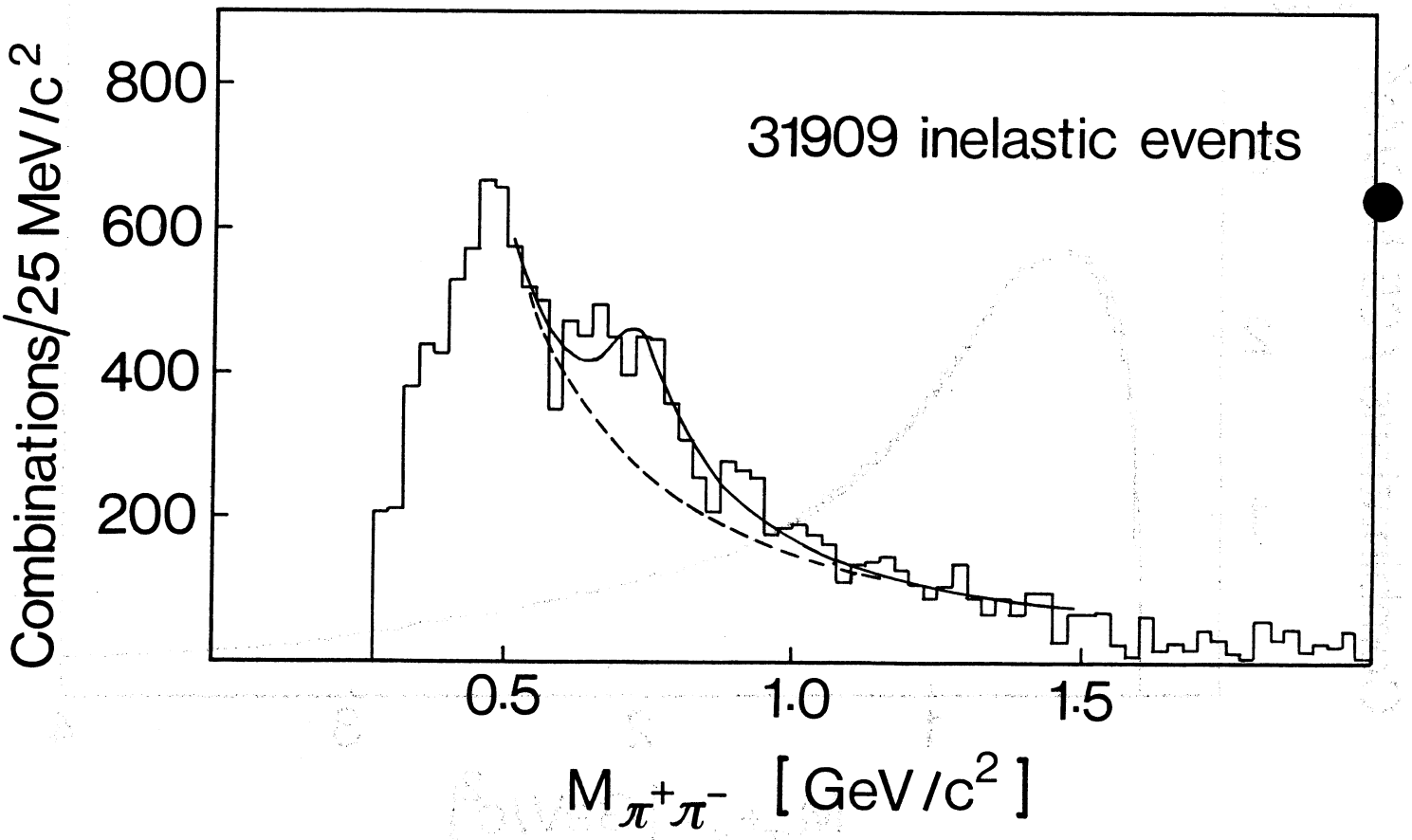
31909 inelastic events
Combinations/25 MeV/c²
800
600
400
200
0.5
1.0
1.5
M π⁺π⁻ [GeV/c²]

Fig. 3a,b

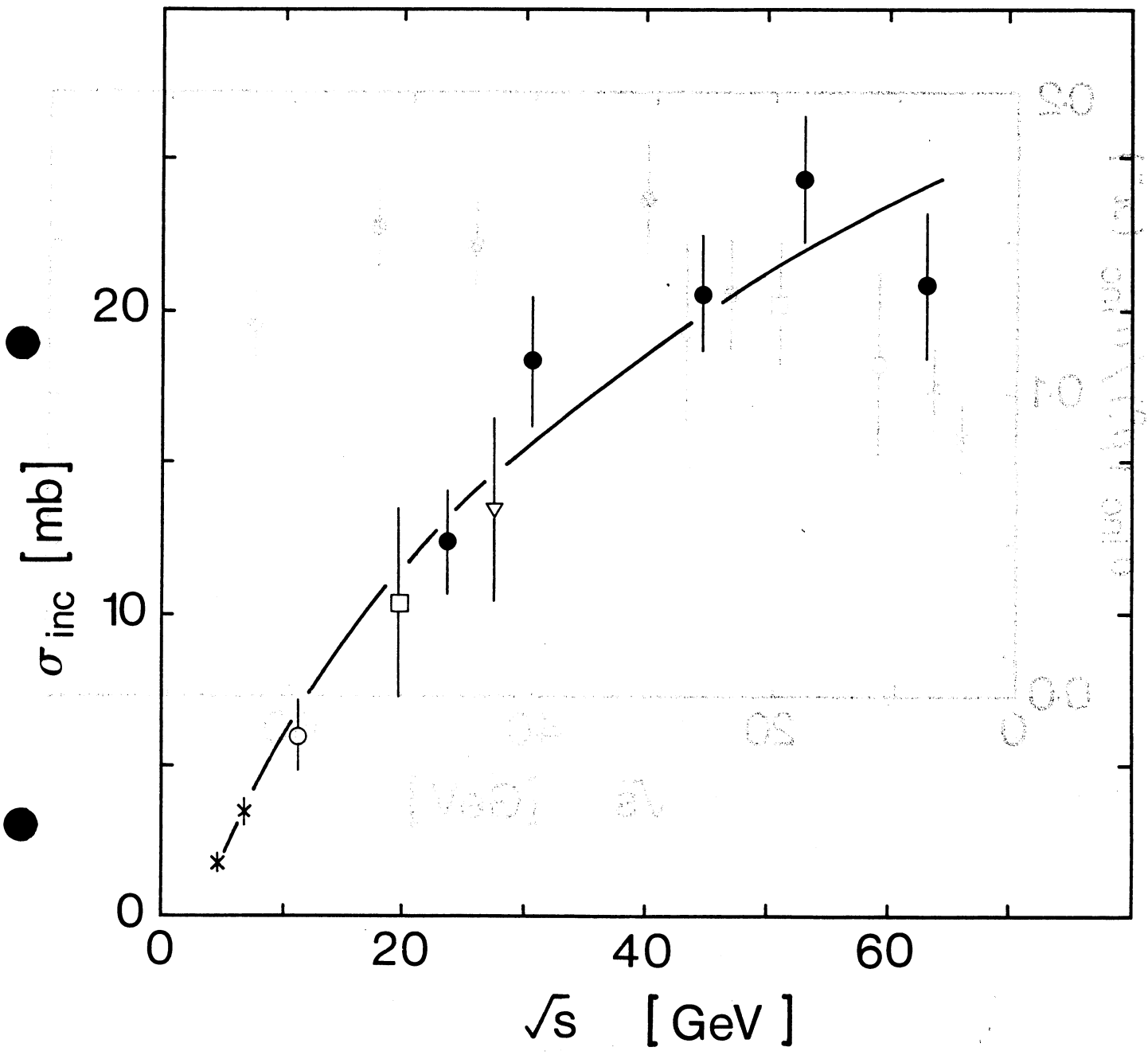

Fig. 3a

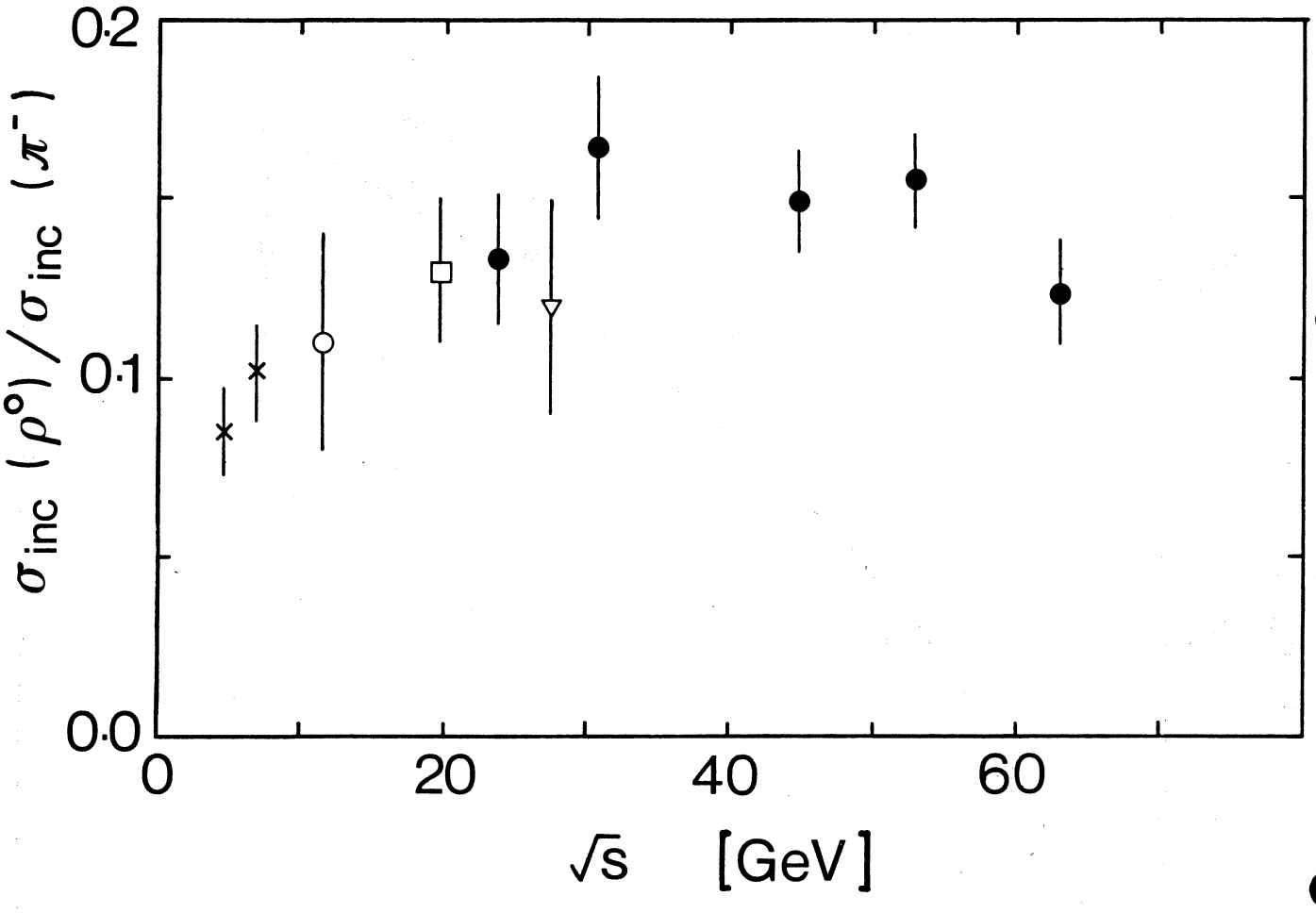

Fig. 5b

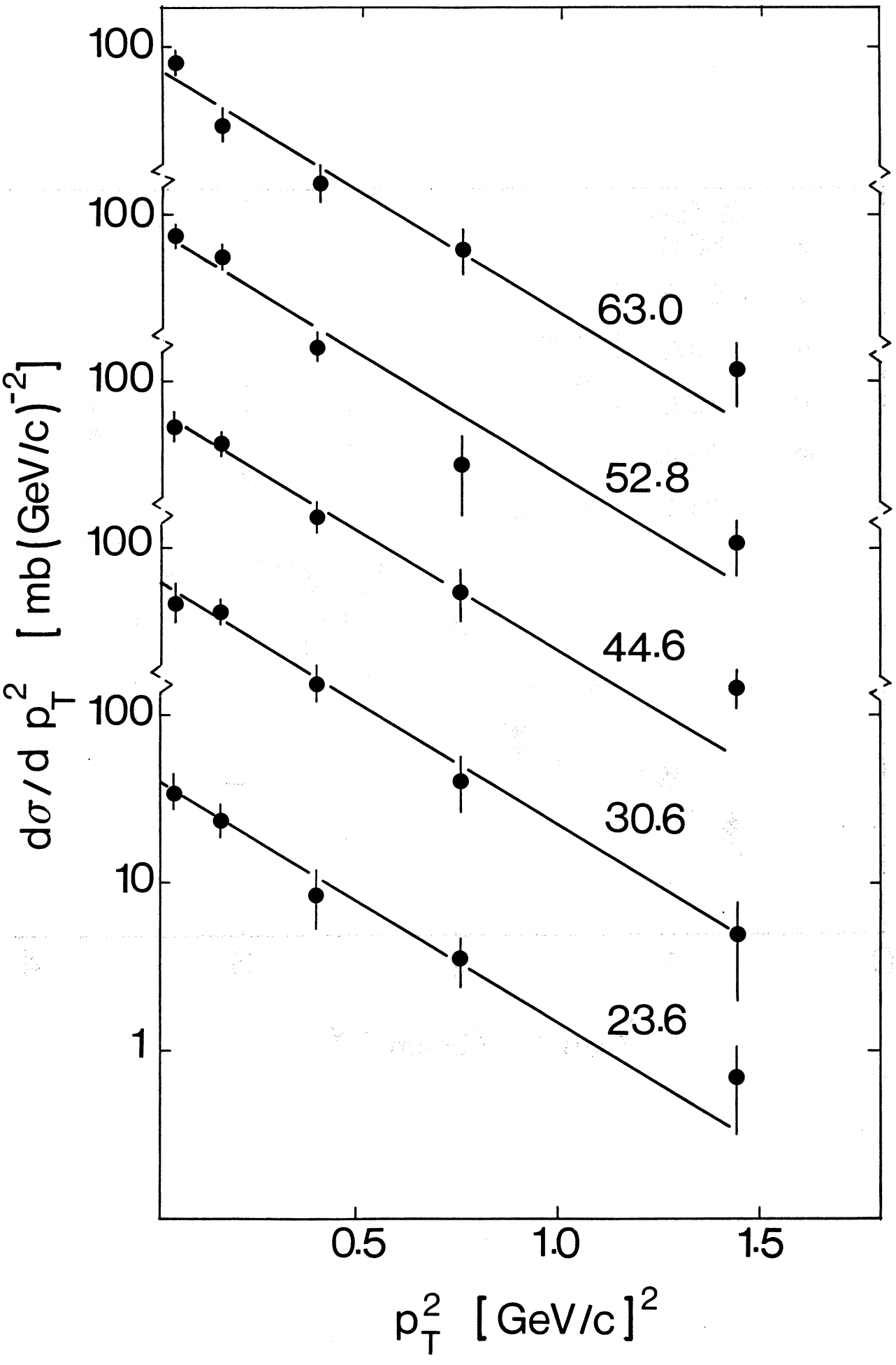
100
100
100
100
100
10
1
63.0
52.8
44.6
30.6
23.6
$d\sigma/d\,p_T^2$ [mb(GeV/c)$^{-2}$]
0.5
1.0
1.5
p_T^2 [GeV/c]^2

Fig. 6

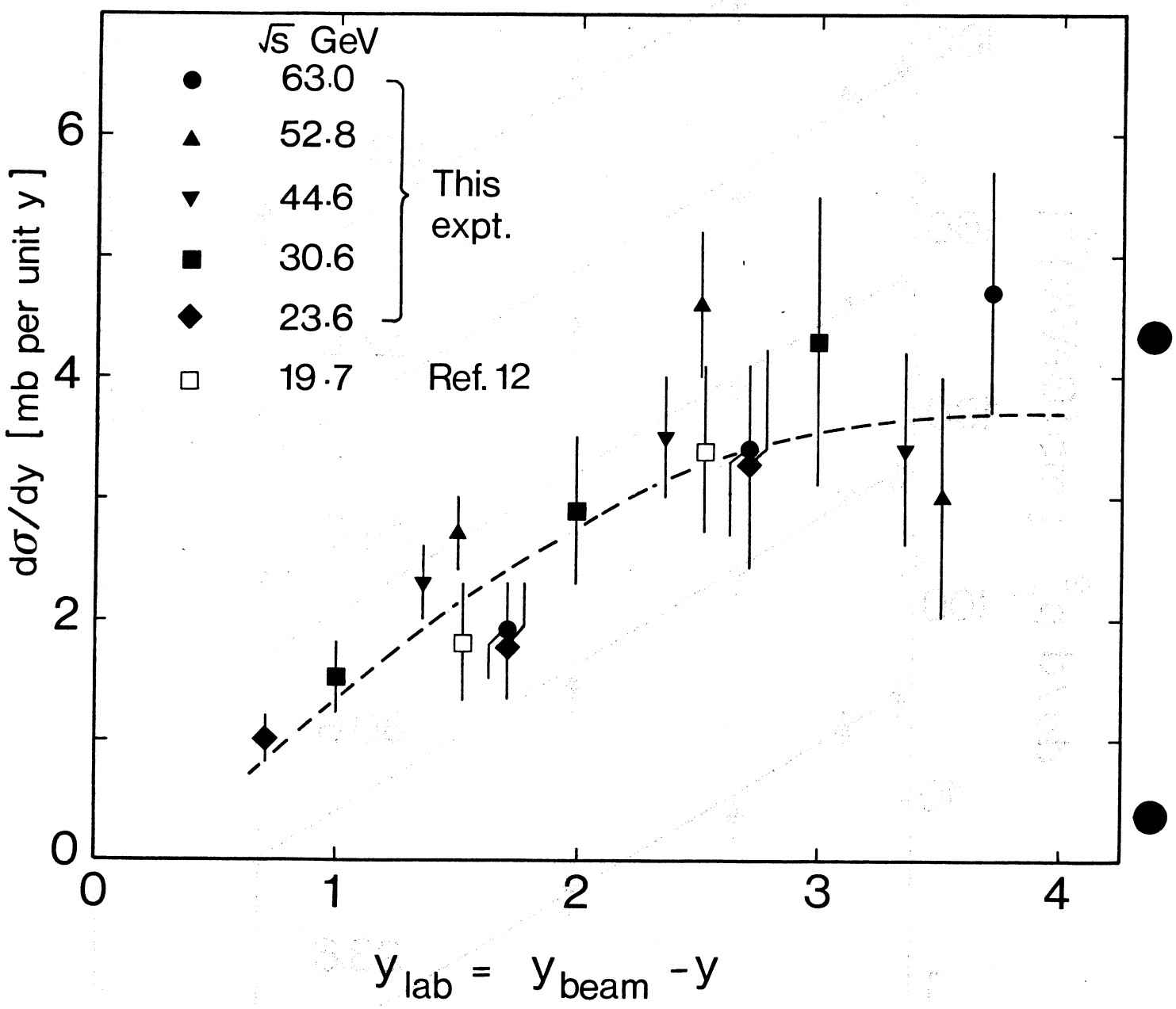
√s GeV
63.0
52.8
44.6
30.6
23.6
This expt.
19.7
Ref. 12
dσ/dy [mb per unit y]
0
2
4
6
0
1
2
3
4
y lab = y beam - y

Fig. 7